

Neutron activation of a multi-chip Silicon-on-Silicon module and its packages

M. Emri¹, A. Fenyvesi², A. Kerek³, J. Molnár², D. Novák²

¹PET Centre, Medical & Health Science Centre, University of Debrecen, Debrecen, Hungary

²Institute of Nuclear Research of the Hungarian Academy of Sciences (ATOMKI), Debrecen, Hungary
(Email: fenyvesi@atomki.hu)

³Royal Institute of Technology(KTH), SCFAB, Stockholm, Sweden

Abstract

Neutron induced activation of a monolithic Application Specific Integrated Circuit (ASIC) and some packagings were studied. It was found that the gamma dose from the activated components of the device could be, on the average, some 10 % of the dose from the external radiation environment at the position of operation of the circuit in Large Hadron Collider (LHC) detectors. At the same time, the auto-radiogram of the neutron activated monolithic ASIC had shown that "hot spots" of induced radioactivity can develop in the structure where the radiation damage hazard can be significantly higher.

I. INTRODUCTION

Components of integrated circuits (chips, substrates, packages, etc.) operating in intense radiation environment in LHC detectors or other high energy physics experiments can be activated significantly by nuclear processes. The induced beta and gamma radiation of the activated components might result in the radiation damage of the circuit even in the case when the LHC beam is not on. The activation can be inhomogeneous inside the device and even local "hot spots" can develop where a significantly increased failure rate can be observed.

In this paper we present results of a detailed study of the neutron-induced activation of a multi-chip Silicon-on-Silicon module (MCM-D) and some packages for it. Our obtained results clearly demonstrate the usefulness of neutron activation studies combined with auto-radiography for identification of radioactive "hot spots" as sources of radiation hazard in MCM-Ds to be used in neutron rich radiation environments like those at LHC experiments.

II. EXPERIMENTAL

The MCM-D (Figure 1) we selected for our studies was originally developed for the digital Front-End and Readout Microsystem (FERMI) by the CERN RD-16 collaboration for

high energy physics calorimetry applications at the LHC. The expected annual neutron flux was 10^{14} n/cm²/year with an additional γ dose up to 1 MRad (10^4 Gy) with exposure time 10^7 s/year. ASICs were flip-chip bonded to the substrate that contained integrated resistors and capacitors. Six different packaging materials and methods [1] were provided by IMM Linköping (Sweden) for possible packing of the FERMI for different applications. Their description is shown in Table 1.

Table 1: Main characteristic data of the irradiated packages and the ASIC chip.

Sample code	Size (mm ²)	No. and type of connections	Main construction materials
IC1	31 x 31	84 connectors	epoxy case Si, Sn, Cu
IC2	31 x 31	84 connectors	epoxy, Au, Si, silica gel coatings glass fibre PC board
IC3	31 x 31	84 connectors	epoxy, Au, Si, epoxy soft coatings, glass fibre PC board
IC2-3	31 x 31	84 connectors	same as IC2 and IC3 without coating glass fibre PC board
IC4	37 x 37	92 pins	polyamid, kovar, Au, Si, Al
IC5	53 x 53	144 pins	ceramic case, kovar, Au
ASIC chip	31 x 31		Si, SiO ₂ , Al, Au

Irradiations were performed at the MGC-20E cyclotron of ATOMKI (Debrecen, Hungary). The neutron source provided neutrons with maximum intensity at around 1 MeV from reactions induced by 18 MeV protons on ⁹Be. The yield of these neutrons is 1.9×10^{10} n/sr/ μ C and the average energy of the emitted neutrons is 3.7 MeV [2]. The MCM-D and the six different packaging samples were irradiated and activated with these neutrons for 14 h. The total fluences were in the range of $(2.3 - 3) \times 10^{13}$ n/cm².

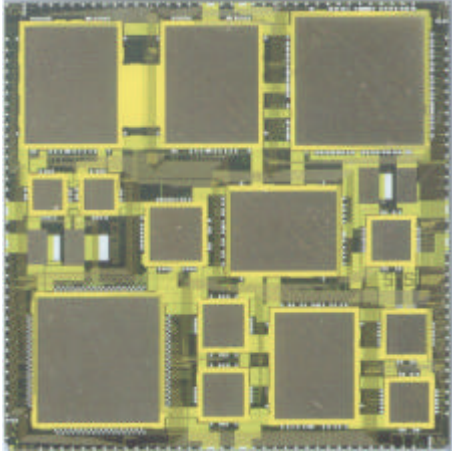


Figure 1: Photograph of a monolithic ASIC for the FERMI module.

After the end of the irradiation, consecutive gamma spectra of the activated packaging samples and the MCM-D were recorded with HPGe detectors. The first measurement was started approximately 5 minutes after the end of irradiation. After gamma counting, the activated MCM-D was put on a storage phosphor screen (Amersham Biosciences Molecular Dynamics, Sunnyvale, CA, USA). The BaFBr:Eu + Polyurethane layer of the screen was excited by both the beta- and gamma-radiation emitted by the sample. The exposition time was 24 hours. After exposition the excited screen was scanned by a laser light and the induced photoluminescence was measured using a Phosphor Imager (Amersham Biosciences Molecular Dynamics, Sunnyvale, CA, USA).

Table 2: Found isotopes and their estimated saturation activities after 1 year of LHC (continuous run of 10^7 sec/year at maximum luminosity) irradiation with 10^{14} neutron/cm² for each packages.

Isotope	T _{1/2}	Activity (Bq)						
		IC1	IC2	IC3	IC2-3	IC4	IC5	ASIC chip
^{106m} Ag	8.5 d	151 +- 28 %	121 +- 31 %	135 +- 25 %	125 +- 29 %	98 +- 21 %	97 +- 25 %	189444 +- 15 %
^{110m} Ag	249.9 d	82 +- 26 %	69 +- 31 %	57 +- 31 %	69 +- 37 %	53 +- 34 %	53 +- 30 %	
¹¹² Ag	3.14 h		116 +- 15 %					
²⁸ Al	2.31 m							
²⁹ Al	6.56 m	1400 +- 14 %			289 +- 13 %			
⁷⁶ As	1.1 d				4.5 +- 60 %			
¹⁹⁶ Au	6.18 d	32 +- 18 %	81 +- 14 %	72 +- 14 %	66 +- 18 %	107 +- 20 %	388 +- 14 %	
^{196m} Au	9.7 h			3.4 +- 55 %	4.2 +- 65 %			
¹⁹⁸ Au	2.697 d	223 +- 13 %	798 +- 12 %	663 +- 11 %	661 +- 12 %	962 +- 14 %	2926 +- 15 %	
¹⁹⁹ Au	3.15 d	35 +- 16 %	9.2 +- 33 %		6.6 +- 46 %	195 +- 26 %		
⁸⁰ Br	17.6 m		5234 +- 13 %					
⁸² Br	1.47 d	214 +- 23 %	630 +- 13 %	529 +- 11 %	521 +- 18 %	639 +- 21 %		
⁵⁷ Co	271.77 d		25 +- 41 %	22 +- 46 %		122 +- 26 %	217 +- 26 %	
⁵⁸ Co	70.78 d		465 +- 23 %	379 +- 17 %	384 +- 16 %	2853 +- 19 %	3339 +- 46 %	
⁶⁰ Co	5.269 y	40 +- 37 %	12 +- 61 %	14 +- 61 %		167 +- 24 %	18 +- 56 %	
^{62m} Co	13.91 m	26 +- 20 %						
⁶⁴ Cu	12.71 h	8570 +- 11 %	975 +- 14 %	853 +- 14 %	815 +- 20 %			
⁵⁹ Fe	45.1 d					105 +- 21 %	8.7 +- 56 %	
²⁷ Mg	9.46 m	197 +- 11 %	487 +- 11 %	295 +- 11 %	482 +- 12 %	12994 +- 11 %	96023 +- 12 %	106 +- 21 %
⁵⁶ Mn	2.576 h		4 +- 60 %	3 +- 65 %	3 +- 65 %	626 +- 13 %	505 +- 13 %	
⁹⁹ Mo	2.78 d						544 +- 20 %	
²⁴ Na	15.06 h	15 +- 30 %	218 +- 11 %	217 +- 11 %	219 +- 11 %	5341 +- 11 %	40845 +- 11 %	16 +- 14 %
⁵⁷ Ni	1.5 d		3 +- 58 %	4 +- 65 %	2.9 +- 65 %	9.1 +- 40 %	317 +- 12 %	
⁶⁵ Ni	2.52 h	176 +- 12 %	20 +- 25 %	17 +- 35 %	20 +- 30 %			
^{120m} Sb	5.8 d	38 +- 20 %						
¹²² Sb	2.70 d	517 +- 18 %						
¹²⁴ Sb	60.2 d	177 +- 40 %						
⁴⁸ Sc	1.82 d	5.9 +- 45 %	3.5 +- 54 %	3.6 +- 60 %	2.6 +- 70 %			0.8 +- 120 %
^{117m} Sn	14 d	72 +- 27 %			3.5 +- 60 %			
¹²³ Sn	129.2 d				125 +- 29 %			
¹²⁵ Sn	9.62 d		75 +- 27 %		69 +- 37 %			
¹⁸⁷ W	23.9 h						4350 +- 15 %	
	Sum:	12 kBq	9.5 kBq	3.5 kBq	4 kBq	25 kBq	150 kBq	190 kBq

III. RESULTS AND DISCUSSION

A. Detailed study of the activation of the MCM-D and some packages for it

The number of induced radioisotopes identified in the evaluated gamma spectra of the packaging samples varied from 13 to 20 (Table 2) depending on the elemental composition of the packages. The range of their half-life extended from 2.3 min to 5.3 year. Their saturation activities were calculated and then they were used to estimate the

activities of the packages expected after 1 year of irradiation with 10^{14} n/cm² at an average neutron flux rate of 10^{14} n/cm²/10⁷ s at the LHC. In Table 3, the most plausible reactions for the found isotopes are listed. As it can be seen from this table, most of the construction elements can be activated through different nuclear processes resulting in final activities with varying half-lives.

It can be concluded from these measurements and calculations that the estimated activities after 1 year of operation of LHC vary over a factor of 40 for the different types of packages studied. For the MCM-D, the expected saturation activity is 190 kBq within the uncertainties of estimation for use at LHC experiments.

Table 3: Nuclear processes giving rise to the activities found

No.	Material	Activation reactions
1.	Aluminium	$^{27}\text{Al}(n, \gamma)^{28}\text{Al}$, $^{27}\text{Al}(n, p)^{27}\text{Mg}$, $^{27}\text{Al}(n, \alpha)^{24}\text{Na}$
2.	Antimony	$^{121}\text{Sb}(n, 2n)^{120\text{m}}\text{Sb}$, $^{121}\text{Sb}(n, \gamma)^{122}\text{Sb}$, $^{123}\text{Sb}(n, 2n)^{122}\text{Sb}$, $^{123}\text{Sb}(n, \gamma)^{124}\text{Sb}$
3.	Bromine	$^{79}\text{Br}(n, \alpha)^{76}\text{As}$, $^{79}\text{Br}(n, \gamma)^{80}\text{Br}$, $^{81}\text{Br}(n, 2n)^{80}\text{Br}$, $^{81}\text{Br}(n, \gamma)^{82}\text{Br}$
4.	Cadmium	$^{106}\text{Cd}(n, p)^{106\text{m}}\text{Ag}$, $^{110}\text{Cd}(n, p)^{110\text{m}}\text{Ag}$, $^{112}\text{Cd}(n, p)^{112}\text{Ag}$
5.	Cobalt	$^{59}\text{Co}(n, p)^{59}\text{Fe}$, $^{59}\text{Co}(n, \alpha)^{56}\text{Mn}$, $^{59}\text{Co}(n, 2n)^{58}\text{Co}$
6.	Copper	$^{63}\text{Cu}(n, \gamma)^{64}\text{Cu}$, $^{65}\text{Cu}(n, 2n)^{64}\text{Cu}$, $^{63}\text{Cu}(n, \alpha)^{60}\text{Co}$, $^{65}\text{Cu}(n, p)^{65}\text{Ni}$
7.	Gold	$^{197}\text{Au}(n, 2n)^{196}\text{Au}$, $^{197}\text{Au}(n, 2n)^{196\text{m}}\text{Au}$, $^{197}\text{Au}(n, \gamma)^{198}\text{Au}$, $^{198}\text{Au}(n, \gamma)^{199}\text{Au}$
8.	Indium	$^{113}\text{In}(n, \alpha)^{110\text{m}}\text{Ag}$, $^{115}\text{In}(n, \alpha)^{112}\text{Ag}$
9.	Iodine	$^{127}\text{I}(n, \alpha)^{124}\text{Sb}$
10.	Iron	$^{54}\text{Fe}(n, \alpha)^{51}\text{Cr}$, $^{56}\text{Fe}(n, p)^{56}\text{Mn}$, $^{58}\text{Fe}(n, \gamma)^{59}\text{Fe}$
11.	Magnesium	$^{24}\text{Mg}(n, p)^{24}\text{Na}$
12.	Manganese	$^{55}\text{Mn}(n, \gamma)^{56}\text{Mn}$
13.	Molybdenum	$^{98}\text{Mo}(n, \gamma)^{99}\text{Mo}$, $^{100}\text{Mo}(n, 2n)^{99}\text{Mo}$
14.	Nickel	$^{58}\text{Ni}(n, 2n)^{57}\text{Ni}$, $^{58}\text{Ni}(n, np)^{57}\text{Co}$, $^{58}\text{Ni}(n, p)^{58}\text{Co}$, $^{60}\text{Ni}(n, p)^{60}\text{Co}$, $^{62}\text{Ni}(n, p)^{62\text{m}}\text{Co}$, $^{62}\text{Ni}(n, \alpha)^{59}\text{Fe}$, $^{64}\text{Ni}(n, \gamma)^{65}\text{Ni}$
15.	Phosphorus	$^{31}\text{P}(n, \alpha)^{28}\text{Al}$
16.	Silicon	$^{28}\text{Si}(n, p)^{28}\text{Al}$, $^{29}\text{Si}(n, p)^{29}\text{Al}$, $^{30}\text{Si}(n, \alpha)^{27}\text{Mg}$
17.	Silver	$^{109}\text{Ag}(n, \gamma)^{110\text{m}}\text{Ag}$
18.	Tellurium	$^{120}\text{Te}(n, p)^{120\text{m}}\text{Sb}$, $^{122}\text{Te}(n, p)^{122}\text{Sb}$, $^{124}\text{Te}(n, p)^{124}\text{Sb}$
19.	Tin	$^{116}\text{Sn}(n, \gamma)^{117\text{m}}\text{Sn}$, $^{117}\text{Sn}(n, n')^{117\text{m}}\text{Sn}$, $^{122}\text{Sn}(n, \gamma)^{123}\text{Sn}$, $^{124}\text{Sn}(n, \gamma)^{125}\text{Sn}$
20.	Titanium	$^{48}\text{Ti}(n, p)^{48}\text{Sc}$
21.	Tungsten	$^{187}\text{W}(n, \gamma)^{187}\text{W}$
22.	Vanadium	$^{51}\text{V}(n, \alpha)^{48}\text{Sc}$

B. Auto-radiogram of the MCM-D irradiated by fast neutrons

In the case of the MCM-D, the gamma counting had shown that ^{24}Na ($T_{1/2} = 14.959$ h) was the far most intense

source of gamma quanta. This isotope was induced by the $^{27}\text{Al}(n, \alpha)^{24}\text{Na}$ nuclear reaction. The decay mode of ^{24}Na is β^- and its Q-value is $Q_{\beta^-} = 5513.6$ keV. Most of the β^- decays of ^{24}Na ($I_{\beta^-} = 99.944$ %) result a β^- -spectrum with $E_{\beta^-} = 1392,91$ keV endpoint energy. Gamma-photons of energy $E_{\gamma} =$

1368.6 keV ($I_\gamma = 100\%$) and $E_\gamma = 2754.5$ keV ($I_\gamma = 99.94\%$) are also emitted.

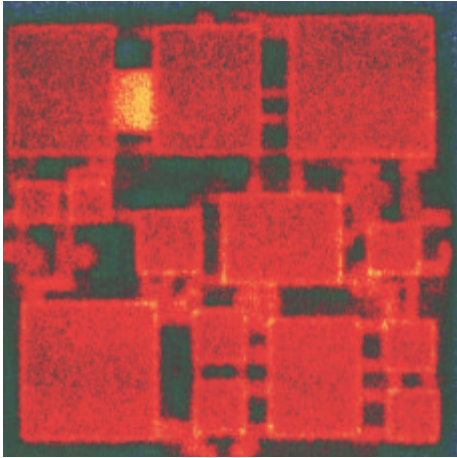


Figure 2: Radiogram of the distribution of the induced gamma activity of the FERMI module irradiated with p+Be neutrons ($E_p = 18$ MeV).

A “hot spot” can be clearly observed in the obtained auto-radiogram (Figure 2). Comparing the auto-radiogram with the photograph of the MCM-D, it can be identified with a dense group of metallic strips between two chips. The material of the strips obviously has high aluminum content.

IV. CONCLUSIONS

For the radiation environment, an expected annual neutron flux of 10^{14} n/cm²/year and γ dose up to 1 Mrad (10^4 Gy) with exposure time 10^7 s/year was considered for the components used in our studies. If one assumes that one third of energy of each decay (mean energy ~ 6 MeV) is absorbed in the silicon chips and substrate of the MCM-D structure (~ 10 g) then some 10 krad 100 Gy) is resulted. In average, it is

approximately 10% additional dose to the 1 Mrad/year (10^4 Gy/year) expected “external” γ -dose.

However, considering the “hot spot” in the auto-radiogram, one can guess that the local dose rate from the radioactivity induced in the dense group of metallic strips can be even significantly higher. The radiation damage hazard for the two neighboring chips is obviously higher than for the other ones in the MCM-D.

It can be concluded that fast neutron activation analyses combined with auto-radiography can provide useful information for assessment of the radiation hazard from induced activation of components of integrated circuits (chips, substrates, packages, etc.) operating in intense radiation environment in LHC detectors or other high energy physics experiments. The method can be applied during the development phase and in failure analyses procedures of installed systems as well.

V. ACKNOWLEDGEMENT

This work was supported in part by the Hungarian Scientific Research Fund (OTKA T026184 and OTKA T034910).

VI. REFERENCES

- [1] M.A. Lone et al., Thick target neutron yield and spectral distributions from the Li-7(p,n), Li-7(d,n), Be-9(p, n), Be-9(d,n) reactions, Nucl. Instr. and Meth. 143 (1977) 331.
- [2] A. Fenyvesi, J. Molnár, A. Kerek, Package irradiation studies, CERN/RD-16, FERMI note 14, January 1993.